Flow Morphology in Planetary Engulfment Events

UC SANTA BARBARA
Kavli Institute for Theoretical Physics

Logan Prust, Lars Bildsten

Kavli Institute for Theoretical Physics

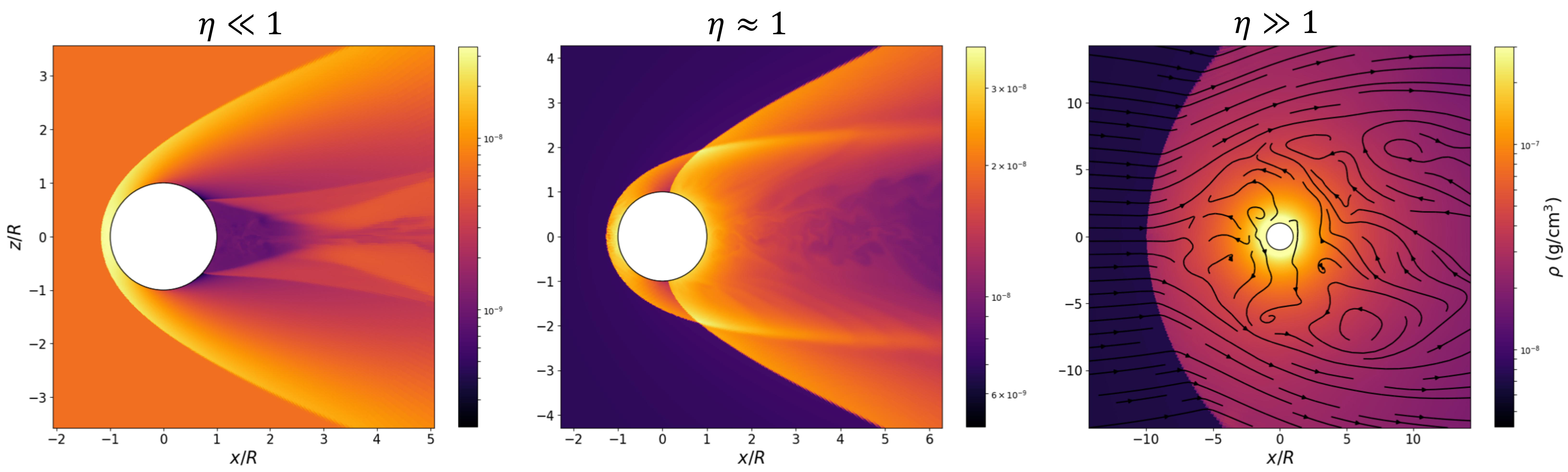

Background

As a star ascends the RGB or AGB, its increase in radius can result in the engulfment of one or more of its inner planets. The planet spirals into the giant due to drag from the envelope, depositing energy which may power a transient event. Massive planets have an immediate dynamical effect on the envelope, driving outflows at tens of km/s [1]. On the other hand, smaller planets are expected to spiral deep into the envelope before being destroyed through either tidal disruption (for planets which fall within tidal radius of the core) or ram-pressure stripping. This energy deposition may cause a thermal pulse, increasing the stellar radius and luminosity, at a galactic rate of ∼0.1 – 1 per year.

A wide range of Mach numbers and regions of stellar structure are experienced by the planet during its inspiral. Upon entering the giant, the planet is highly supersonic ($\mathcal{M} \approx 5$), quickly decreasing to near sonic velocity before eventually being destroyed near the base of the convective envelope. Knowledge of the interactions between the planet and envelope over this parameter space is key to understanding these events.

Numerical Setup

We simulate planetary engulfment using the Athena++ adaptive mesh refinement code [2], modeling only the immediate vicinity of the planet. This "wind-tunnel" approach is possible because the planet is in general not massive enough to significantly alter the global structure of the envelope due to the high mass ratio. The surface of the planet with radius R and mass m is treated as a reflective boundary, and the surrounding gas is set to conditions typical of an AGB envelope. We perform a suite of simulations, varying both the Mach number $\mathcal{M}$ and the accretion radius

$$R_A = \frac{2Gm}{v^2}$$

of the planet to cover the relevant parameter space. Because the cooling time of the shock-heated material surrounding the planet is longer than the inspiral time, we do not expect significant accretion, but the accretion radius is nonetheless useful as a measure of the strength of gravity relative to inertial forces. These quantities then define the "non-linearity parameter"

$$\eta = \frac{1}{2}\frac{\mathcal{M}^2}{\mathcal{M}^2 - 1}\frac{R_A}{R},$$

which we find to be an important metric in characterizing the flow morphology.

Flow Morphology

Each simulation is run until it reaches steady state, which takes approximately one fluid crossing time of the domain. We find that the flow morphology is determined by the value of η, with two distinct regions separated by a transition region at $\eta = 1$, as shown in the figure above.

Separation Bubble ($\eta \ll 1$):

Here the morphology resembles that of the non-gravitating case. A bow shock forms near the planet surface, with a small region of subsonic flow near its nose. In the outer wings of the shock, the post-shock flow remains supersonic, and accelerates as it flows around the sides of the planet until it separates from the surface. This separation is facilitated by a recompression shock, turning the flow so that a low-density bubble of material forms directly behind the planet. The gas in this "separation bubble" is very subsonic and high entropy, and is separated from the rest of the flow by a contact discontinuity known as a slip line.

Transition Region ($\eta \approx 1$):

When η is near unity, the gravitational influence of the planet is significant, but still struggles to compete with the high ram pressure of the oncoming gas. The flow upstream of the planet is similar to the low η case, while downstream the planet is able to more effectively retain the gas in its wake. The separation bubble is hydrostatically supported, allowing it to be much larger than in the non-gravitating case. Thus, the extent of the bubble along the surface of the planet is also larger, forcing the recompression shock forward so that it intersects with the bow shock.

Hydrostatic Halo ($\eta \gg 1$):

For high η, gravity is strong enough to cloak the planet in a large halo of gas. Here the bow shock is far from the planet, and the recompression shock is absent entirely. The halo is found to be largely in hydrostatic equilibrium, though there are small fluid velocities present. The halo is also isentropic, with entropy equal to the post-shock value. Streamlines upstream of the shock are deflected toward the radial direction due to gravity, and as such the strength of the shock is fairly uniform along a large portion of the shock. The result is that the entropy generation of this portion of the shock is also fairly uniform, in contrast to the non-gravitating case.

Dynamical Friction

The dynamical friction on a supersonic body can in general be expressed as

$$F_{\rm DF} = 4\pi\rho\left(\frac{Gm}{v}\right)^2 \ln\left(\frac{s_{\rm max}}{s_{\rm min}}\right),$$

where the Coulomb logarithm depends on the effective linear size of the body $s_{\rm min}$ and the maximum extent of the wake $s_{\rm max}$. Though our wind-tunnel simulations are ill-equipped to determine the extent of the wake, they are ideal for studying $s_{\rm min}$, which depends only on the flow near to the body. For large η, we find that $s_{\rm min}$ is nearly equal to the shock stand-off distance R_s, in agreement with previous work [3]. For low η, we find that $F_{\rm DF}$ depends both on R_s and on the accretion radius. Specifically, we propose the new formula

$$\frac{s_{\rm min}}{R_s} = \begin{cases} 2R/R_A = (\eta\cos^2\mu)^{-1} & \eta \le 1 \\ 1 & \eta > 1. \end{cases}$$

Here the alternate form for $\eta \le 1$ is obtained using the definitions of η and the Mach angle μ.

Pressure Drag

For large η, the hydrostatic halo exerts a uniform pressure over the planet surface. However, for low η the non-uniform distribution leads to a net force. The separation bubble exerts a significant pressure on the downstream side of the planet ($\theta > 90°$) which can rival the ram pressure on the upstream side ($\theta < 90°$).

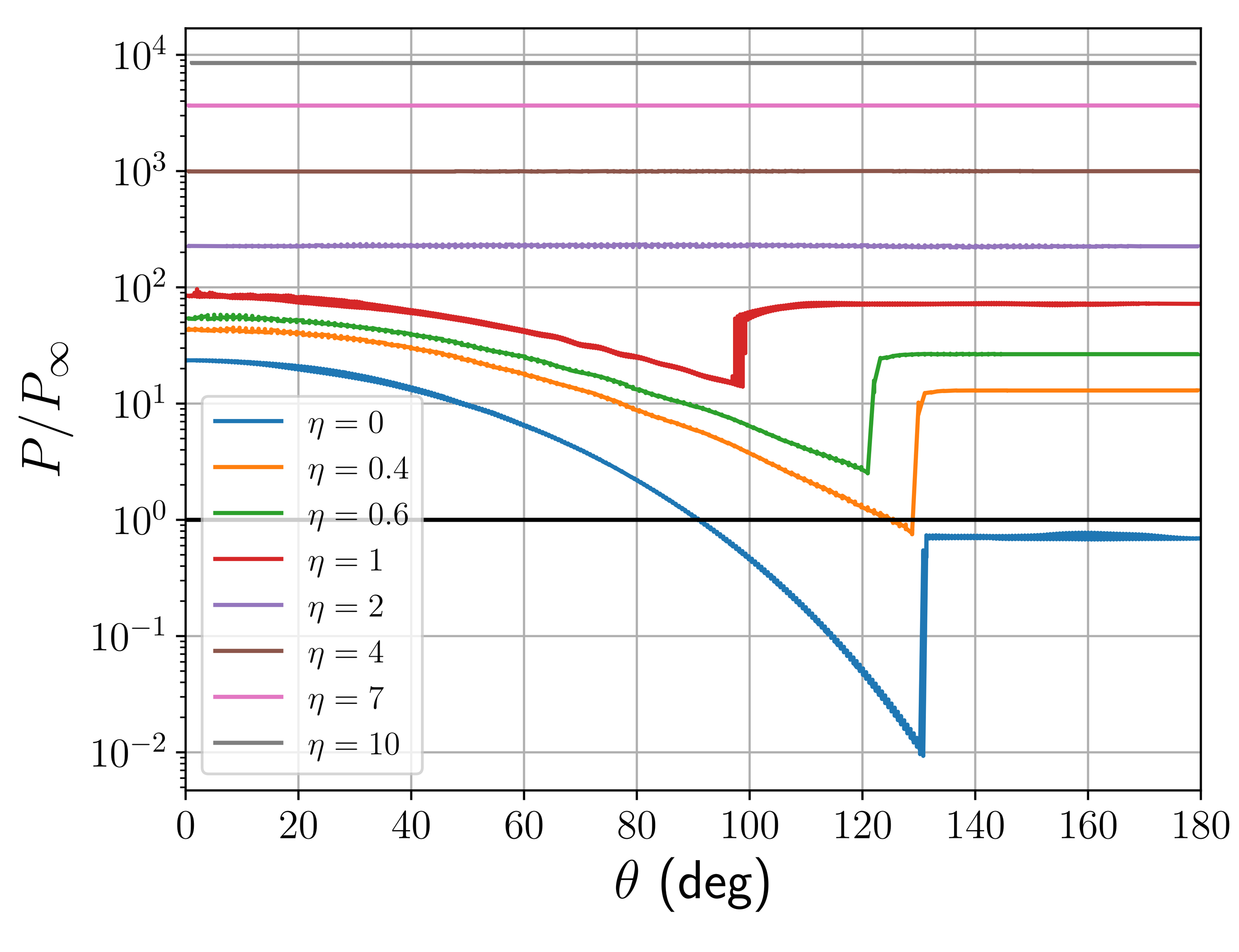

References

[1] Kishalay De et al.
An infrared transient from a star engulfing a planet.
Nature, 617:55–60, May 2023.

[2] James M. Stone, Kengo Tomida, Christopher J. White, and Kyle G. Felker.
The athena adaptive mesh refinement framework: Design and magnetohydrodynamic solvers.
The Astrophysical Journal Supplement Series, 249(1):4, June 2020.

[3] Daniel Thun, Rolf Kuiper, Franziska Schmidt, and Wilhelm Kley.
Dynamical friction for supersonic motion in a homogeneous gaseous medium.
Astronomy and Astrophysics, 589:A10, May 2016.

ljprust@kitp.ucsb.edu